A novel yellow emitting phosphor Dy^{3+}, Bi^{3+} co-doped YVO_4 potentially for white light emitting diodes*

Ci Zhi-Peng(慈志鹏)[a], Wang Yu-Hua(王育华)[a)b)†], and Zhang Jia-Chi(张加弛)[a]

[a] *Department of Material Science, School of Physical Science and Technology, Lanzhou University, Lanzhou* 730000, *China*
[b] *Key Laboratory for Magnetism and Magnetic Materials of the Ministry of Education, Lanzhou University, Lanzhou* 730000, *China*

(Received 5 May 2009; revised manuscript received 20 November 2009)

Novel $Y_{1-x-y}VO_4$:xDy^{3+}, yBi^{3+} ($0.01 \leq x \leq 0.05, 0 \leq y \leq 0.20$) phosphors for light emitting diode (LED) were successfully synthesised by solid-state reaction. The calculation results of electronic structure show that YVO_4 has a direct band gap with 3 eV at G. The top of the valence band is dominated by O 2p state and the bottom of the conduction band is mainly composed of O 2p and V 3d states. An efficient yellow emission under near-ultraviolet (365 nm) excitation is observed. Compared with the pure YVO_4:Dy^{3+} samples, the Dy^{3+}, Bi^{3+} co-doped samples show a more intensive emission peak (at 574 nm) and a new broad emission band (450–770 nm), due to the $^4F_{9/2} - {}^6H_{13/2}$ transition of Dy^{3+} and the emission of the VO_4^{3-}–Bi^{3+} complex respectively. The optimum chromaticity index of $Y_{1-x-y}VO_4$:xDy^{3+}, yBi^{3+} ($0.01 \leq x \leq 0.05, 0 \leq y \leq 0.20$) is (0.447, 0.497), which indicates that YVO_4:Dy^{3+}, Bi^{3+} has higher colour saturation than the commercial phosphor YAG: Ce^{3+}. The effects of concentration of Dy^{3+}, Bi^{3+}, electric states and the photoluminescence properties are discussed in details.

Keywords: phosphor, light-emitting diode, vanadate
PACC: 7855, 7860

1. Introduction

The attraction of solid state lighting for general purposes is due to the increasing demand for more efficient power usage. Light-emitting diodes (LEDs) are one option for efficient lighting since their power consumption is low, their durability is high, and their lifetimes are long. They are also more environmentally conscientious than other sources such as compact fluorescents since they contain no mercury. Commercially one method of producing white light with LEDs is colour mixing by using two or more LED dies.[1–5] Another method is to downconvert the emission from a blue or ultraviolet LED to a longer-wavelength light using phosphors. By far the most common and simple LED-based white light source is a configuration with a 450–470 nm blue nitride LED and a yellow-emitting phosphor which usually made of cerium doped yttrium aluminum garnet (YAG:Ce^{3+}).[6–10] But this white light LED fabricated with YAG: Ce^{3+} cannot create warm white light due to the phosphor emitting greenish yellow light. This problem would be solved by combining another red phosphor or developing a novel long-wavelength yellow phosphor.

It is well known that YVO_4:Re^{3+}had been intensively studied for many years for their application in UV excitation due to the efficient energy transfer from the vanadate group (VO_4^{3-}) to Re^{3+}.[11–14] These phosphors give off intense emission under UV excitation. The YVO_4 is of a zircon-type structure, which is built from chains of alternating edge-sharing VO_4 and YO_8.[15] Thus the Re^{3+} could be firmly coordinated by eight O^{2-} in YVO_4 when it substitutes for Y^{3+}. As a result, YVO_4:Re^{3+} (such as YVO_4:Eu^{3+})[16] shows not only desirable absorption in UV region but also excellent thermal and chemical stability. The luminescent materials doped with Dy^{3+}[17–19] have been used as potential efficient phosphors due to its two dominant emission bands in the blue region (470–500 nm) and yellow region (560–600 nm).[12] The Bi^{3+}-containing rare-earth materials have been also explored because the $6s^2$–6s6p excitations of Bi^{3+} can efficiently harvest the near-UV light.[20–23] In various host material, Bi^{3+} is usually used as a sensitizer due to the efficient energy transition from Bi^{3+} to Re^{3+}.[24,25] So we expect that Bi^{3+} could also transfer efficiently energy to Dy^{3+} in the YVO_4 host. In this work, the $Y_{1-x-y}VO_4$:xDy^{3+},

*Project supported by the National Natural Science Foundation of China (Grant No. 10874061).
†Corresponding author. E-mail: wyh@lzu.edu.cn
© 2010 Chinese Physical Society and IOP Publishing Ltd

yBi^{3+} ($0.01 \leq x \leq 0.05$, $0 \leq y \leq 0.20$) phosphors are successfully synthesized and its electric structure and luminescent properties are investigated in details.

2. Experimental

$Y_{1-x-y}VO_4$:xDy^{3+}, yBi^{3+} ($0.01 \leq x \leq 0.05$, $0 \leq y \leq 0.20$) phosphors were prepared by solid-state reaction. The starting materials were Y_2O_3(4N), V_2O_5(A.R.), Bi_2O_3(A.R.) and Dy_2O_3(4N). A stoichiometric amount of the above oxides were weighed and mixed together in an agate mortar, and finely ground. The samples were heated in an alumina crucible (in air) at 800 °C for 1h and then at 1000 °C for 12 h, then we obtained the samples required.

All the samples were characterised by powder x-ray diffraction (XRD) using a Rigaku diffractometer with Ni-filtered Cu Kα radiation. The absorption edges of the products were determined from the onsets of diffuse reflectance spectra of the samples measured by an UV–vis spectrophotometer (PE lambda950) using $BaSO_4$ as a reference. The photoluminescence spectra were measured by a Xe lamp (FLS-920T). All the luminescence spectra were recorded at room temperature.

The calculation of the electronic structure for YVO_4 was carried out with density functional theory and performed with the CASTEP code.[26,27] The local-density approximations (LDA) were chosen for the theoretical basis of density function. Two steps were necessary for calculating the electronic band structure of YVO_4. The first step was to optimise their crystal structure using the crystallographic data reported in the literature.[28] There is only a small difference between the experimental lattice parameters and calculated ones after the optimisation of crystal structure, which will not be indicated here. The second step was to calculate the band structure and density of states of YVO_4 for the optimised structure. Lattice parameters and atomic coordinates were fixed at the values obtained by the crystal structure optimisation process in the first step. For the two steps, the basic parameters were chosen as follows in setting up the CASTEP run: the kinetic energy cutoff = 300 eV, k-point spacing = 0.5 Å^{-1} (1 Å=0.1 nm), sets of k points = 3×3×3 for YVO_4, SCF tolerance thresholds = 2.0×10^{-6} eV/atom, and space representation = reciprocal.

3. Results

The x-ray powder diffraction patterns show that all samples are of a single phase. As an example, the powder XRD patterns of $Y_{0.97-x}VO_4$:0.03Dy^{3+}, xBi^{3+} ($0 \leq x \leq 0.20$) are shown in Fig. 1. According to the JCPDS card 72-0861, all peaks can be well indexed with space group of $I4_1$/amd141 (a = 0.7123 nm, c = 0.6292 nm). As indicated in Fig. 1, the doped Dy^{3+} and Bi^{3+} have a slight influence on the host YVO_4 tetragonal structure. With the incorporation of Dy^{3+} and Bi^{3+} into the YVO_4 lattice, the XRD patterns peaks slightly shift to smaller angles. By the Bragg's law, $2d\sin\theta = n\lambda$, where d is the planar spacing for the diffracting planes, it is indicated that the co-doping with Dy^{3+} and Bi^{3+} increases the lattice parameters of the phosphor, due to the fact that the ionic radius of Y^{3+} (0.088 nm) is slightly lower than those of Dy^{3+} (0.091 nm) and Bi^{3+} (0.096 nm).

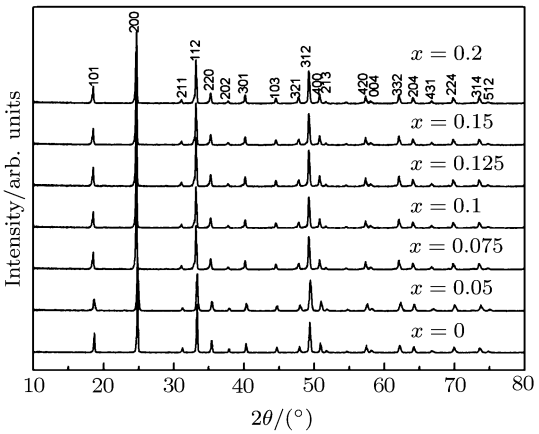


Fig. 1. The XRD patterns of $Y_{0.97-x}Bi_xDy_{0.03}VO_4$ samples ($0 \leq x \leq 0.20$).

Figure 2 displays the band structures of YVO_4. YVO_4 shows a direct optical band gap and the gap between the lowest energy of the conduction band and the highest energy of the valence band is about 3 eV, which is lower compared to the experimentally determined values (about 3.7 eV, see Fig. 6). This difference is normal as the LDA underestimates the size of the band gap.[29] Figure 3 shows the total and partial density of states of YVO_4. The top of the valence band is dominated by O 2p state. The bottom of the conduction band is mainly composed of O 2p and V 3d states.

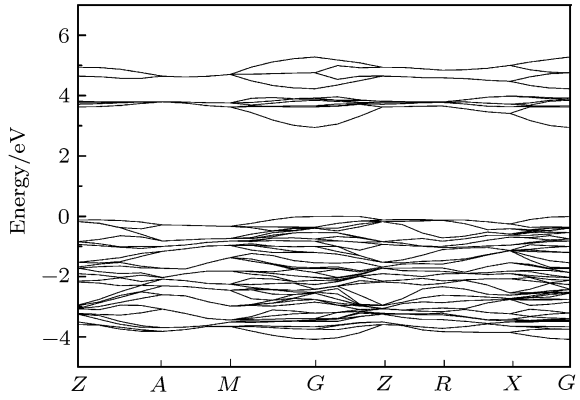


Fig. 2. Band structures of YVO_4.

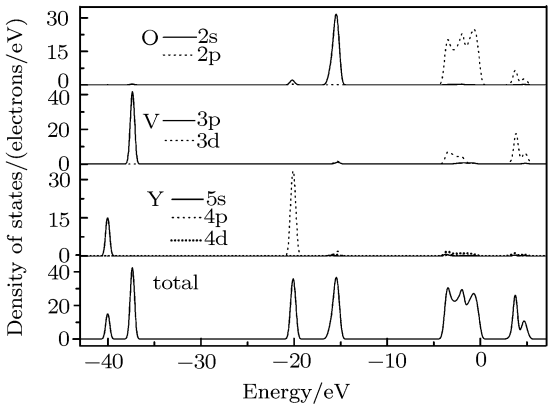


Fig. 3. Total and partial density of states of YVO_4.

All the $Y_{1-x}VO_4$:xDy^{3+} ($0.01 \leq x \leq 0.05$) excitation spectra have the similar features. As an example, Fig. 4 shows the representative excitation spectrum of $Y_{0.97}VO_4$:0.03Dy^{3+}. The spectrum contains

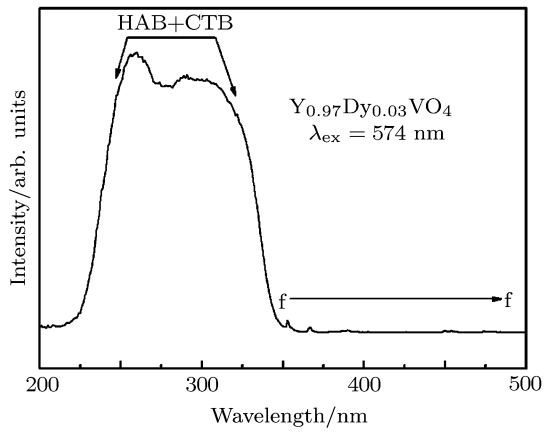


Fig. 4. The excitation spectrum of $Y_{0.97}VO_4$:0.03Dy^{3+}.

some broad bands in the wavelength region of 210–340 nm. It can be attributed to the host absorption band (HAB) and the charge transfer band (CTB) of Dy^{3+}O^{2-}.[14] In the longer wavelength (350–500 nm), the weaker sharp peaks is from the f–f transitions of the Dy^{3+} with 4f^9 electron configuration.[30] The peaks at 352 nm, 365 nm, 389 nm and 450 nm are due to the $^6H_{15/2} - {}^4M_{15/2} + {}^6P_{7/2}$, $^6H_{15/2} - {}^4I_{11/2}$, $^6H_{15/2} - {}^4M_{19/2} + {}^4M_{11/2}$ and $^6H_{15/2} - {}^4G_{11/2}$ transition of Dy^{3+} respectively.[31]

The emission spectrum of $Y_{0.97}VO_4$:0.03Dy^{3+} is shown in Fig. 5. The spectral peaks at 483 nm (blue colour) and 573 nm (yellow colour) corresponding to $^4F_{9/2} - {}^6H_{15/2}$ and $^4F_{9/2} - {}^6H_{13/2}$ transitions of Dy^{3+} have been observed under 365 nm excitation. The dominant peak (573 nm) is due to the Dy^{3+} $^4F_{9/2} - {}^6H_{13/2}$ hypersensitive transition ($\Delta J = 2$). On the one hand, the $^4F_{9/2} - {}^6H_{15/2}$ transition is magnetically allowed and hardly varies with the crystal field strength around the Dy^{3+}. On the other hand, Y^{3+} is located at a site (D_{2d}) deviated from an inverse centre in the host of YVO_4. When Dy^{3+} replaced the site of Y^{3+}, Dy^{3+} is located at a site of D_{2d}, which is deviated from an inverse centre in the host of YVO_4. The $^4F_{9/2} - {}^6H_{13/2}$ transition is a forced electric dipole transition being allowed only at low symmetries with no inversion center.[32] So the intensity of the yellow emission (573 nm) is stronger than that of the blue one. The emission intensity at 573 nm of Dy^{3+} was also investigated as a function of Dy^{3+} concentration in YVO_4 phosphor in the inset of Fig. 5. It is found

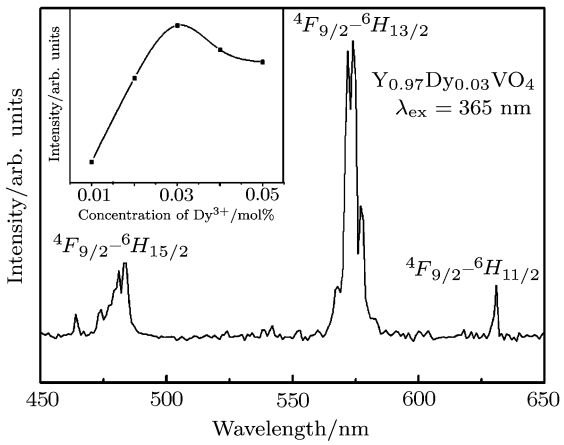


Fig. 5. The emission spectrum of $Y_{0.97}VO_4$:0.03Dy^{3+}; the inset for the variation of the luminescent intensity with Dy^{3+} concentration in the system $Y_{1-x}VO_4$:xDy^{3+} ($0.01 \leq x \leq 0.05$).

that the PL emission intensity of Dy^{3+} increases with the increase of the concentration of Dy^{3+}, reaching a maximum value at 3 mol% for Dy^{3+}, and then decreases when the concentration of Dy^{3+} is larger than 3mol%. This is because of a well-known phenomenon

of concentration quenching[32] in rare earth-doped system due to mutual $Dy^{3+}-Dy^{3+}$ interactions. So the Dy^{3+}-doped concentration of $Y_{1-x-y}VO_4$:xDy^{3+}, yBi^{3+} ($0.01 \leq x \leq 0.05$, $0 \leq y \leq 0.20$) samples in next work is fixed to 3 mol%.

The diffuse reflectance spectra of YVO_4 and $Y_{0.87}VO_4$:$0.03Dy^{3+}$, $0.1Bi^{3+}$ are shown in Fig. 6. For the undoped sample, a strong absorption shows up in the range of about 200–340 nm caused by the electronic transition of the host. The optical band gap E_g of YVO_4 determined by extrapolating the linear portion of the reflection curve onto energy (wavelength) is about 3.7 eV. For the Dy^{3+}, Bi^{3+}-codoped sample, the absorption edge shifts to the longer wavelength side. A new strong absorption band centred at 365 nm is present, which can be dominantly assigned to the absorption of $VO_4^{3-}-Bi^{3+}$. The optical band gap E_g of $Y_{0.87}VO_4$:$0.03Dy^{3+}$, $0.1Bi^{3+}$ is about 3.3 eV and the result is consonant with the excitation spectrum of $Y_{0.87}VO_4$:$0.03Dy^{3+}$, $0.1Bi^{3+}$.

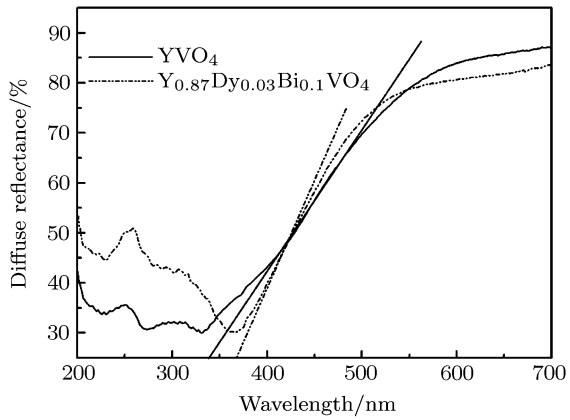


Fig. 6. Diffuse reflection spectra of undoped YVO_4 and $Y_{0.87}VO_4$:$0.03Dy^{3+}$, $0.1Bi^{3+}$ samples.

The excitation spectrum in pure YVO_4 doped with Dy^{3+} shows a broad absorption with a band edge at 340 nm. In the case of $Y_{0.97-x}VO_4$:$0.03Dy^{3+}$, xBi^{3+}, the band edge shifts from 340 nm to 380 nm with increasing Bi^{3+} concentration (see Fig. 7). This shift occurs due to a certain charge-transfer character in the lower optical transitions of the $VO_4^{3-}-Bi^{3+}$ complex, i.e. a 6s electron of Bi^{3+} is promoted into the empty d shell of the V^{5+}. The hole in the excited state is not longer localized on the oxygen ligands alone, but also on the s^2 ions of Bi^{3+}. As a consequence the optical transitions are at lower energies.[33] With increasing Bi^{3+} concentration, the ${}^6H_{15/2} - {}^4M_{15/2} + {}^6P_{7/2}$ (352 nm) and ${}^6H_{15/2} - {}^4I_{11/2}$ (365 nm) transitions of Dy^{3+} are intensely increased; however, the host absorption band and the charge transfer band are strongly decreased in Fig. 7. It could be explained by the energy transition from $VO_4^{3-}-Bi^{3+}$ complex to Dy^{3+} that is more efficient than that from VO_4^{3-} to Dy^{3+}. Correspondingly it is found that the intensity of the ${}^6H_{15/2} - {}^4I_{11/2}$ (365 nm) transition of Dy^{3+} is enhanced gradually with increasing Bi^{3+} concentration, and the optimal concentration of Bi^{3+} is 10 mol%. When the concentration x of the doped Bi^{3+} exceeds 10%, the excitation intensity at 365 nm decreases gradually because of the concentration quenching effect.

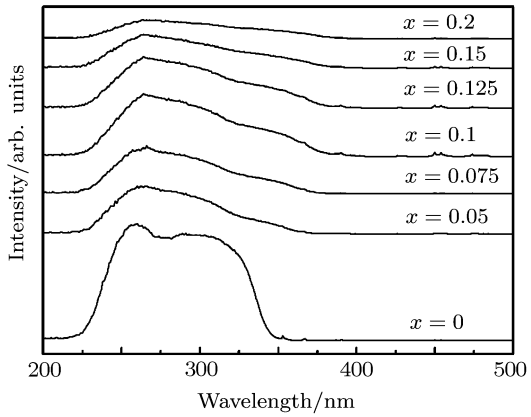


Fig. 7. The excitation spectra of $Y_{0.97-x}VO_4$:$0.03Dy^{3+}$, xBi^{3+} ($0 \leq x \leq 0.2$, $\lambda_{em} = 574$ nm).

Figure 8 shows the emission spectrum of $Y_{0.87}VO_4$:$0.03Dy^{3+}$, $0.1Bi^{3+}$ and the variation of the luminescence intensity with Bi^{3+} concentration in the system $Y_{0.97-x}VO_4$:$0.03Dy^{3+}$, xBi^{3+} ($0 \leq x \leq 0.20$). Under the excitation of 365 nm, it can be clearly seen that the emission spectrum of $Y_{0.87}VO_4$:$0.03Dy^{3+}$, $0.1Bi^{3+}$ contains two emission peaks and a broad band. The two emission peaks centred at 483 and 574 nm correspond to the characteristic emission of Dy^{3+} due to the transitions of ${}^4F_{9/2} - {}^6H_{15/2}$ and ${}^4F_{9/2} - {}^6H_{13/2}$ respectively. The broad yellow emission in the range of 450–770 nm is ascribed to the emission of $VO_4^{3-}-Bi^{3+}$.[34–38] The highest emission intensity of $Y_{0.97-x}VO_4$:$0.03Dy^{3+}$, xBi^{3+} at 574 nm ($x = 0.10$, $\lambda_{ex} = 365$ nm) is as 14 times high as that of the $Y_{0.97}VO_4$:$0.03Dy^{3+}$. In addition, compared with the commercial phosphor YAG: Ce^{3+}, the emission of $Y_{0.87}VO_4$:$0.03Dy^{3+}$, $0.1Bi^{3+}$ phosphors occurs at fairly longer wavelength.

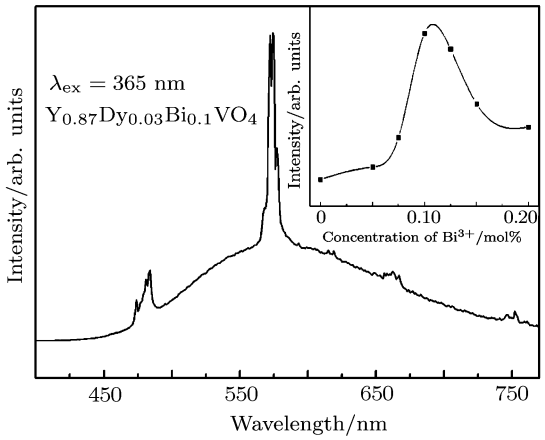


Fig. 8. The emission spectrum of $Y_{0.87}VO_4$:0.03Dy^{3+}, 0.1Bi^{3+}; the inset shows the variation of the emission intensity as a function of Bi^{3+} content x in the system $Y_{0.97-x}VO_4$:0.03Dy^{3+}, xBi^{3+} ($0 \le x \le 0.20$).

The luminescent colour is an important factor for application of phosphors. Thus the emission colours of YVO_4:0.03Dy^{3+}, $Y_{0.87}VO_4$:0.03Dy^{3+} 0.1Bi^{3+} and YAG:Ce^{3+} are analysed and confirmed with the help of CIE (Commission Internationale de l'Eclairage) chromaticity coordinates diagram. The colour coordinates of YVO_4:0.03Dy^{3+}, $Y_{0.87}VO_4$:0.03Dy^{3+} 0.1Bi^{3+} and YAG:Ce^{3+} are shown in Fig.9. The CIE coordinates are (0.401, 0.438), (0.447, 0.497) and (0.41, 0.56) corresponding to YVO_4:0.03Dy^{3+}, $Y_{0.87}VO_4$:0.03Dy^{3+}, 0.1Bi^{3+} and YAG: Ce^{3+}, respectively. It is clear that colour coordinates of the as-synthesised samples fall in the yellow region and shift towards pure yellow with the doping of Bi^{3+}. Compared with the commercial phosphor YAG: Ce^{3+} whose CIE colour coordinates are in greenish yellow region, the phosphor of $Y_{0.87}VO_4$:0.03Dy^{3+} 0.1Bi^{3+} has high colour saturation.

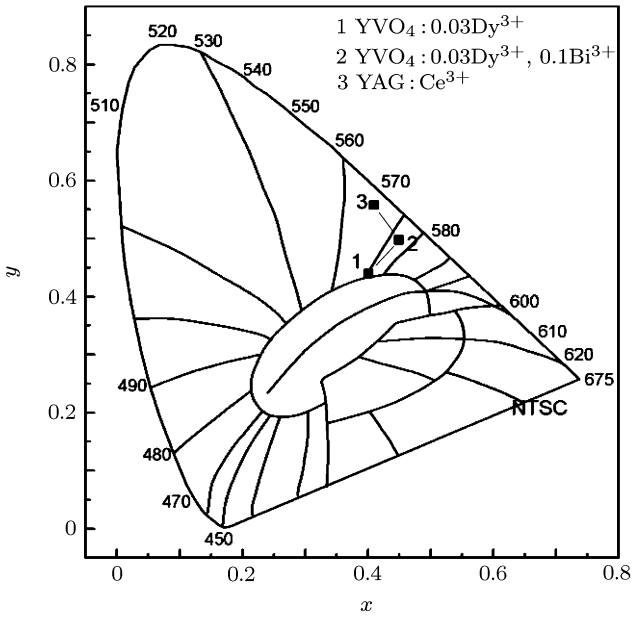


Fig. 9. CIE of YVO_4:0.03Dy^{3+}, $Y_{0.87}VO_4$:0.03Dy^{3+}, 0.1Bi^{3+} and YAG: Ce^{3+}.

4. Conclusions

Novel yellow phosphors $Y_{1-x-y}VO_4$:xDy^{3+}, yBi^{3+} ($0.01 \le x \le 0.05$, $0 \le y \le 0.20$) have been successfully obtained by solid-state reaction. The YVO_4:0.03Dy^{3+} sample shows a broad excitation band in the range of 210–340 nm (λ_{em} = 574 nm) and a weak emission (λ_{ex} = 365 nm). With the co-doping of Bi^{3+}, the change of transition broad band edge shifts to longer wavelength (380 nm) dominantly due to the absorption of the VO_4^{3-}–Bi^{3+} complex. The ${}^6H_{15/2} - {}^4M_{15/2} + {}^6P_{7/2}$ (352 nm) and ${}^6H_{15/2} - {}^4I_{11/2}$ (365 nm) transition of Dy^{3+} are also intensely enhanced due to the efficient energy transition from the VO_4^{3-}–Bi^{3+} to Dy^{3+}. The phosphors $Y_{1-x-y}VO_4$: xDy^{3+}, yBi^{3+} ($0.01 \le x \le 0.05$, $0 \le y \le 0.20$) show excellent yellow emission and the optimal luminescence property for $x = 0.03$, $y = 0.10$. The emission intensity of $Y_{0.87}VO_4$:0.03Dy^{3+}, 0.1Bi^{3+} is as 14 times strong as that of the $Y_{0.97}VO_4$:0.03Dy^{3+}. Compared with the commercial phosphor YAG:Ce^{3+} whose CIE colour coordinates are (0.41, 0.56), $Y_{0.87}VO_4$:0.03Dy^{3+}, 0.1Bi^{3+} (0.447, 0.497) has higher colour saturation. Therefore, Dy^{3+}, Bi^{3+} co-doped YVO_4 phosphor would have the great potential application in white LEDs.

References

[1] Li P L, Yang Z P, Wang Z J and Guo Q L 2008 *Chin. Phys.* B **17** 1907

[2] Chen X B, Zhang G Y, Chen J K, Wang H, Liu Y B, Shang M R and Li J W 1993 *Chin. Phys.* **2** 695

[3] Zhang L, Guo X, Liang T, Gu X L, Lin M and Shen G D 2007 *J. Microelectron.* **38** 1

[4] Wei X D, Cai L Y, Lu F C, Chen X L, Chen X Y and Liu Q L 2009 *Chin. Phys.* B **18** 3555

[5] Wang Z J, Yang Z P, Guo Q L, Li P L and Fu G S 2009 *Chin. Phys.* B **18** 2068

[6] Yang Z P, Li X, Yang Y and Li X M 2007 *J. Lumin.* **707** 122
[7] Yao G Q, Duan J F, Ren M, Yu H D and Lin J H 2001 *J. Lumin.* **21** 22
[8] Xia G D, Zhou S M, Zhang J Jand Xu J 2005 *J. Cryst. Growth.* **357** 279
[9] Li P L, Yang Z P, Wang Z J and Guo Q L 2008 *Chin. Phys.* B **17** 1135
[10] Ma M X, Zhu D C and Tu M J 2009 *Acta Phys. Sin.* **58** 5826 (in Chinese)
[11] Wang Y H, Sun Y K, Zhang J C, Ci Z P, Zhang Z Y and Wang L 2008 *Physica* B **403** 2071
[12] Neeraj S, Kijima N and Cheetham A K 2004 *Solid State Communications* **131** 65
[13] Vengala Rao B and Buddhudu S 2008 *Materials Chemistry and Physics* **1** 65
[14] Yan B and Su X Q 2006 *Journal of Non-Crystalline Solids* **352** 3275
[15] Zhang H W, Fu X Y, Niu S Y, Sun G Q and Xin Q 2007 *Materials Letters* **61** 308
[16] Kong J H, Im W B, Lee D C, Kim J Y, Jeon D Y, Kang Y C and Jung K Y 2005 *Solid State Commun.* **133** 651
[17] Seeta Rama Raju G, Park J Y, Jung H C, Yang H K, Moon B K, Jeong J H and Kim J H 2009 *Optical Materials* **31** 1210
[18] Lakshminarayana G, Yang Hucheng and Qiu Jianrong 2009 *Journal of Solid State Chemistry* **182** 669
[19] Jia G, Song Y H, Yang M, Huang Y J, Zhang L H and You H P 2009 *Optical Materials* **31** 1032
[20] Gerner P, Kramer K and Gudel H U 2003 *J. Lumin.* **112** 102
[21] Setlur A A and Srivastava A M 2006 *Optical Materials* **29** 410
[22] Chen L, Zheng H W, Cheng J G, Song P, Yang G T, Zhang G B and Wu C 2008 *Journal of Luminescence* **128** 2027
[23] Kumar Vinay, Kumar Ravi, Lochab S P and Singh Nafa 2007 *Nuclear Instruments and Methods in Physics Research* B **262** 194
[24] Zeng X Q, Im S J, Jang S H, Kim Y M, Park H B, Son S H, Hatanaka H, Kim G Y and Kim S G 2006 *J. Lumin.* **121** 1
[25] Liu X M and Lin J 2007 *J. Lumin.* **700** 122
[26] Segall M, Linda P, Probert M, Pickard C, Hasnip P, Clark S and Payne M 2002 Materials Studio CASTEP, version 2.2; (Accelrys: San Diego, CA)
[27] Segall M, Linda P, Probert M, Pickard C, Hasnip P, Clark S and Payne M 2002 *J. Phys.: Condens. Mater.* **14** 2717
[28] Baglio, Sovers J A and J O 1971 *Journal of Solid State Chemistry.* **3** 458
[29] Jones R O and Gunnarsson O 1989 *Rev. Mod. Phys.* **61** 689
[30] Su X Q and Yan B 2006 *Journal of Alloys and Compounds* **421** 273
[31] Zhang H W, Fu X Y, Niu S Y and Xin Q 2008 *Journal of Alloys and Compounds* **457** 61
[32] Zhang J C and Wang Y H 2008 *Chin. Phys. Lett.* **25** 1453
[33] Blasse G and Bril A 1968 *J. Chem. Phys.* **48** 217
[34] Moncorg R and Boulon G 1979 *J. Lumin.* **376** 18
[35] Blasse George 1980 *The Luminescence of Closed-shell Transition-metal Complexes* pp.32–35 (Heidelberg, Berlin: Springer)
[36] Lee S K, Chang H J, Han C H, Kim H J, Jang H G and Hee D P 2001 *Journal of Solid State Chemistry* **156** 267
[37] Wang S F, Gu F, Lu M K, Zou W G, Liu S W, Xu D, Yuan D R and Zhou G J 2004 *Journal of Physics and Chemistry of Solids* **65** 1243
[38] Zhang Q H, Wang J, Yu R J, Zhang M and Su Q 2008 *Electrochem. Solid-State Lett.* **11** 335